HARD X-RAY SOURCE MOTIONS IN THE 2002 JULY 23 GAMMA-RAY FLARE

SÄM KRUCKER, G. J. HURFORD, AND R. P. LIN

Space Sciences Laboratory, University of California at Berkeley, Grizzly Peak at Centennial Drive, Berkeley, CA 94720-7450; krucker@ssl.berkeley.edu

ABSTRACT

The *Reuven Ramaty High Energy Solar Spectroscopic Imager* (*RHESSI*) is used to study the hard X-ray (HXR) source motions of the 2002 July 23 γ-ray flare. Above 30 keV, at least three HXR sources are observed during the impulsive phase that can be identified with footpoints of coronal magnetic loops that form an arcade. On the northern ribbon of this arcade, a source is seen that moves systematically along the ribbon for more than 10 minutes. On the other ribbon, at least two sources are seen that do not seem to move systematically for more than half a minute, with different sources dominating at different times. The northern source motions are fast during times of strong HXR flux but almost absent during periods with low HXR emission. This is consistent with magnetic reconnection if a higher rate of reconnection of field lines (resulting in a higher footpoint speed) produces more energetic electrons per unit time and therefore more HXR emission. The absence of footpoint motion in one ribbon is inconsistent with simple reconnection models but can be explained if the magnetic configuration there is more complex.

Subject headings: acceleration of particles — Sun: flares

1. INTRODUCTION

Solar hard X-ray (HXR) bremsstrahlung from energetic electrons accelerated in the impulsive phase of a flare is observed to be primarily from the footpoints of magnetic loops. The mechanism that accelerates these particles is still not understood. Standard magnetic reconnection models predict increasing separation of the footpoints during the flare (e.g., Priest & Forbes 2002) as longer and larger loops are produced. If the reconnection process results in accelerated electrons (Øieroset et al. 2002), the HXR footpoints should show this motion. The motion is only apparent; it is due to the HXR emission shifting to footpoints of neighboring newly reconnected field lines. Hence, the speed of footpoint separation reflects the rate of magnetic reconnection and should be roughly proportional to the total HXR emission from the footpoints. Sakao, Kosugi, & Masuda (1998) analyzed footpoint motions in 14 flares observed by *Yohkoh* hard X-ray telescope but did not find a clear correlation between the footpoint separation speed and the HXR flux. Recently, however, source motion seen in Hα was studied by Qiu et al. (2002). They found some correlation with HXR flux during the main peak but not before and after.

The *Reuven Ramaty High Energy Solar Spectroscopic Imager* (*RHESSI*; Lin et al. 2002) allows HXR footpoint motion to be studied in detail. First results from Fletcher & Hudson (2002) analyzing several *GOES* M-class flares show systematic but more complex footpoint motions than a simple flare model would predict. In this Letter, the HXR source motion in the 2002 July 23 γ-ray flare is investigated (see Lin et al. 2003 for an overview). The very long duration of HXR footpoint emission of over 10 minutes makes this event favorable for studying footpoint motion. A rough correlation between HXR footpoint separation and the total HXR flux is found.

2. OBSERVATIONS

During the impulsive phase (00:27–00:40 UT), at least three HXR sources can be distinguished above 30 keV in the cleaned images with the highest resolution (clean beam size of 3″.3 FWHM; Fig. 1, *top*): a northern source (f1) in a positive polarity region and a southern (f2) source and a third source in between

(f3) in a negative polarity region. Furthermore, each of these sources has counterparts seen in EUV and Hα. The EUV and Hα observations show a two ribbon structure, with the HXR source f1 on the northern ribbon and f2 and f3 on the southern ribbon (White et al. 2003). Thus, these HXR sources appear to be at footpoints of coronal magnetic loops; this is confirmed by Michelson Doppler Imager (MDI) observations of white-light emission from the same three sources. The similar temporal variations of f1 and f2 in their light curves as well as in their spectra (Emslie et al. 2003) indicate that they are at opposite ends of the same magnetic loop. The magnetic connection between source f3 and the other footpoints is unclear at the present stage of data analysis; f3 shows less spectral variation, and its light curve stops being similar to f1 and f2 after 00:30:30 UT, disappearing entirely after ∼00:34 UT. Below 30 keV, a coronal source dominates the HXR emission (Lin et al. 2003). During the impulsive phase, this source has a thermal spectrum with temperatures around 40 MK (Emslie et al. 2003), i.e., a "superhot" coronal source (Lin et al. 1981).

2.1. *Source Motion*

Cleaned images (pixel size of 0″.25) in the 30–80 keV range with a clean beam size of 4″.8 FWHM (grids 2–8 were used) with time resolution of 26 and 8 s were used to study the source motions. Not including grid 1 improved the image quality slightly and still allowed a clear separation of the different sources. For each source, a two-dimensional noncircular Gaussian fit around the maximum was used to determine the source centroid location to an accuracy below the chosen pixel size.

Figure 2 shows that the northern footpoint (f1) moves in a linear motion roughly parallel to the apparent neutral line along the ribbon with a velocity up to ∼50 km s^{-1}. The velocities along and perpendicular to the line of motion are derived by differentiation using three-point Lagrangian interpolation. Since the direction of motion is roughly along constant longitude, projection effects are small along the direction of the main motion but could be significant perpendicular to it. However, the observed motion perpendicular is very small (Fig. 3); during the first minutes no perpendicular motion is seen, with a standard deviation of ∼0″.08 for the 26 s cadence images
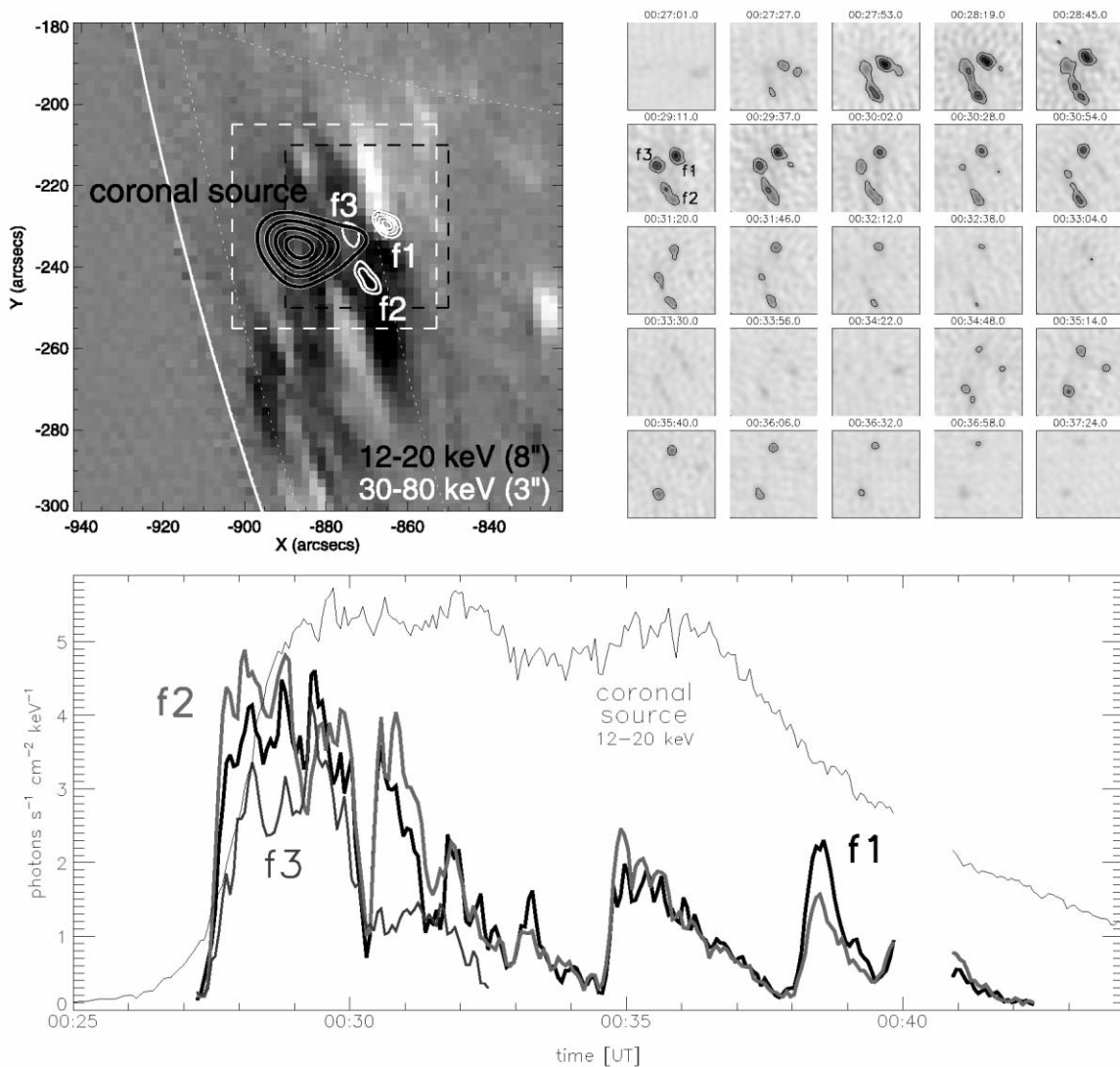
Fig. 1.—Location and temporal variation of the different HXR sources seen during the main phase of the γ-ray flare of 2002 July 23. *Top left*: The three main footpoint sources f1, f2, and f3 (*white contours*; 30–80 keV, clean beam size of 3″.3 FWHM) and the coronal source (*black contours*; 12–20 keV, clean beam size of 9″.6 FWHM) taken at 00:28:15 UT are superposed on the preflare MDI magnetogram (00:12 UT). Contour levels are 30%, 50%, 70%, and 90% of the maximum emission. The white box marks the field of view of the images shown in Fig. 2. *Top right*: Cleaned images (30–80 keV, clean beam size of 3″.3 FWHM) taken with 26 s integration time. The shown field of view of 40″ × 40″ with the center pixel at (−870, −235) is marked in black in the image to the left. Images are scaled to the maximum emission in the time series. For a clearer representation, contour levels at 20%, 50%, and 80% of the absolute maximum of the same images are shown as well. *Bottom*: Time profiles of individual footpoints at 30–80 keV (*thick curves*) and the coronal source at 18–25 keV (*thin curves*; divided by 1500) taken from images at 4 s cadence.

(~0″.16 for the 8 s cadence). This standard deviation is used as an upper limit for the uncertainty in the centroid location in Figure 3. The centroids of the 26 and 8 s cadence images agree well (Fig. 3, *left and middle*); however, details of sudden movements (best seen at 00:30:28, 00:31:48, and 00:38:12 UT) are lost in the 26 s cadence data. These sudden jumps often occur at times near the rise of individual HXR peaks. The velocities derived from the 8 s cadence images are therefore somewhat higher, while some peaks in the 26 s cadence data are less pronounced (e.g., 00:38:12 UT) or even averaged out (e.g., 00:30:28 UT). MDI white-light observations mentioned earlier show the same source motion as seen in HXR but with less accuracy and at lower cadence. The Hα observations show a more complex source than seen in HXR but also reveal a similar source motion.

The other footpoints located on the southern ribbon do not move in the same way. The southern source (f2) shows a more complex, elongated source structure sometimes even showing a double peak (e.g., image at 00:28:45 UT in Fig. 1, *top left*). A more detailed analysis is needed to determine the significance of this double structure. The centroid position of f2 is plotted in Figure 2 (*left*). During the first minutes (00:27–00:34 UT), f2 is mostly dominated by emission around (−870, −245). For times with a double source, it occasionally happens that the maximum emission is coming from the other source slightly (~4″) to the northeast. However, no systematic source motion is seen. With the later peaks after 00:35 UT, the centroid of f2 is at a significantly different position, toward the east (for simplicity, this source is still labeled f2 although it might be independent of the earlier source f2). Also during this later time, no clear systematic source motion is seen; the averaged source location is around (−874.9, −239.8) with a standard deviation of 0″.6. The third source, f3, does not show systematic motion in the same direction for more than half a minute at a time,
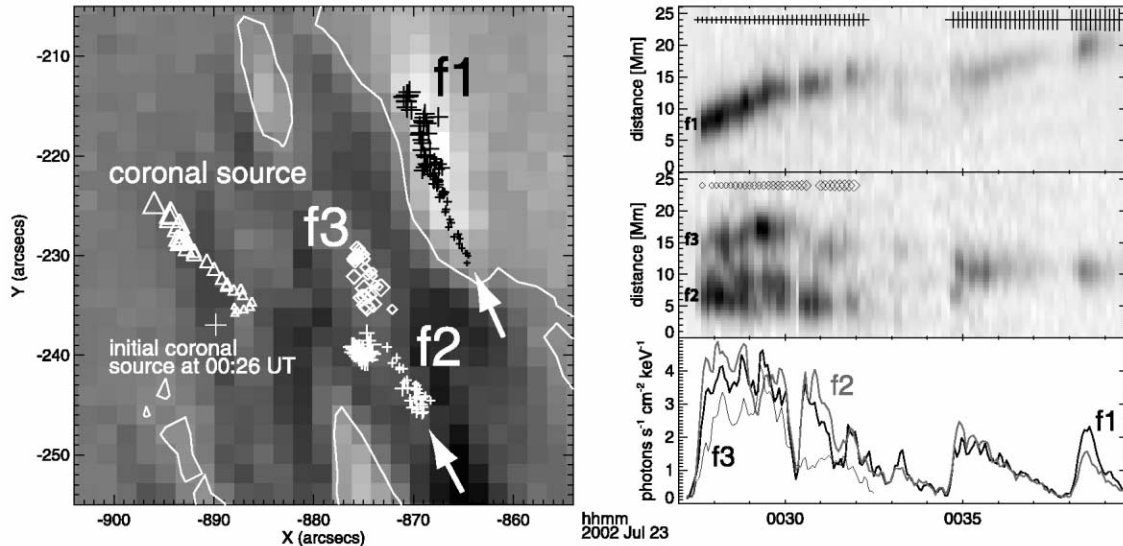
FIG. 2.—*Left*: Temporal evolution of the HXR footpoints f1 (*black plus signs*), f2 (*white plus signs*), and f3 (*white diamonds*) at 30–80 keV and the coronal source (*white triangles*) at 18–25 keV. The centroid positions of the different sources taken every 8 s for the footpoints and every 26 s for the coronal source are shown on an MDI magnetogram in which the apparent neutral line is shown in white; extreme values are ±600 G (cf. Fig. 1, *top right*). The increasing size of the symbols represents times from 00:26:35 to 00:39:07 UT. The centroid of the initial coronal source at 00:26 UT is marked with a white plus sign. *Right*: HXR profiles along the two ribbons at 30–80 keV (*top and middle panel*) and along the main direction of motion of the coronal source at 18–25 keV (*bottom*). Black is enhanced emission. The directions corresponding to these profiles are given by arrows in the image on the left.

but the centroids are also roughly located along the ribbon. During the time of the strongest emission (00:29–00:30 UT), f3 stays fixed around $(-875.6, -230.0)$ within a standard deviation of $0''.2$.

The gradual superhot coronal source moves in a similar direction as the northern footpoint (f1) with a comparable speed (Fig. 3, *right*). Before 00:28:30 UT, an initially coronal non-thermal source (Lin et al. 2003) dominates; afterward, the newly emerging superhot coronal emission dominates, resulting in an apparent shift of the observed centroid locations toward the superhot source. After 00:28:30 UT, the actual source motion of the superhot source is seen.

The motion of the northern footpoint f1 clearly correlates with the time profile of the HXR footpoint (Fig. 3). During the initial

peaks in HXR (00:27:30–00:29:30 UT), the source motion is fast. Around the dip in HXR flux at 00:30:20 UT, the motion is very slow or even absent. Then it increases again during the following HXR peak at 00:30:40 UT. For the following minutes with relatively low HXR emission, f1 moves slowly and even seems to stop between 00:33:00 and 00:34:30 UT. Then, with the new HXR peak at 00:35 UT, it starts moving again, although with a delay of ~30 s. After ~00:36 UT, it slows down before it increases again during the HXR peak around 00:38:30 UT. In the velocities derived from 26 s cadence data, there is a rough correlation between the absolute values of the velocities and the total HXR flux. However, the relation between the velocities and the HXR flux is not linear; the fluxes of the larger peaks between 00:27 and 00:30 UT are almost three times the fluxes of later peaks
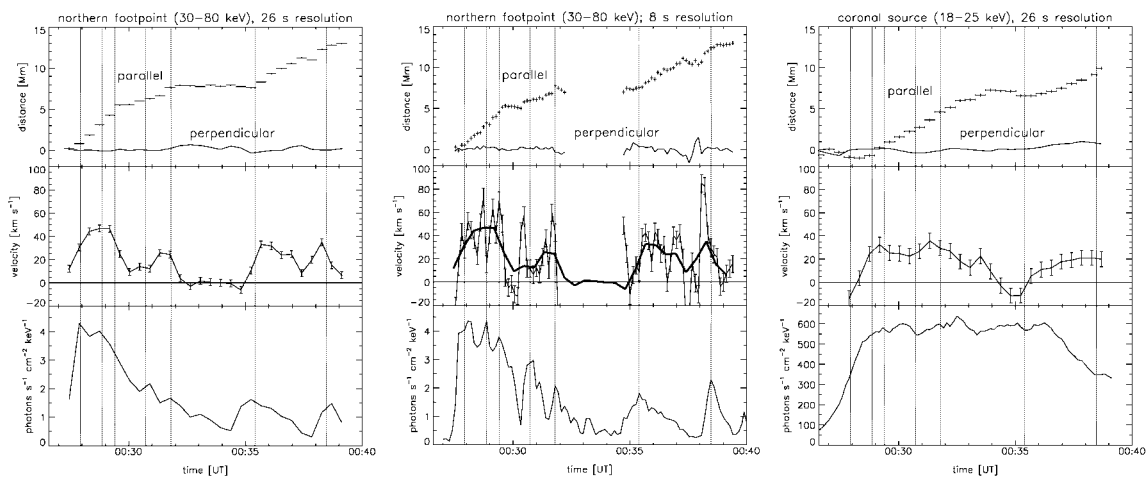

FIG. 3.—Motion of the northern footpoint f1 (in 26 s resolution on the left and 8 s resolution in the middle) and the coronal source (26 s resolution). For each of the three plots, three panels are shown: the traveled distance parallel and perpendicular to the main direction of motion (*top*; cf. Fig. 2, *left*), the velocity along the main direction of motion (*middle*), and the total flux (*bottom*). For temporal comparison, vertical gray lines mark the times of HXR peaks selected from the 8 s resolution time profile. Because of the lower statistics in the 8 s resolution images, a clear source location could not be determined for all times, and so some data points are missing. The derived velocities from the 26 s cadence images are also shown as a thick black line in the figure for the 8 s data for comparison.

after 00:34 UT, but the observed velocities are only slightly smaller for the later weaker peaks. The velocities derived from the 8 s data reveal more detail, showing that the source motion is often largest in the rise to the peak (best seen at 00:30:28, 00:31:48, and 00:38:12 UT).

3. DISCUSSION

The *RHESSI* HXR observations of the 2002 July 23 γ-ray flare show footpoint emissions above 30 keV originating from the ribbons of a magnetic arcade, whereas a coronal source dominates below 30 keV. One footpoint source (f1) moves systematically for more than 10 minutes, but others do not. This is not what would be expected from simple reconnection models but is consistent with earlier findings (e.g., Sakao 1994; Fletcher & Hudson 2002). The measured velocities of up to ~50 km s^{-1} are comparable to the values reported by Sakao, Kosugi, & Masuda (1998). The superhot coronal source moves with a similar speed and in a similar direction as the moving footpoint (f1). Contrary to simple reconnection models, the direction of motion is roughly along the ribbon and not perpendicular to it. This indicates that the reconnected magnetic field lines are highly sheared. The continuous motion along a straight line suggests that footpoints of the newly reconnected loops in the northern ribbon just lie next to the previously reconnected loop.

The lack of systematic footpoint motion for more than half a minute in the other ribbon implies a much more complicated magnetic configuration of the field lines connecting the reconnection site and the footpoints. One end of the newly reconnected field lines may not be simply rooted adjacent to the previously flaring footpoint, but might be connected to a different location along the ribbon. Hence, the observed HXR source does not show systematic motion; instead, it occasionally jumps to a different location. The magnetic field at the southern ribbon is indeed complex, as revealed by the MDI magnetogram, while the northern ribbon shows a smaller sized, simply shaped positive polarity region.

Thus, we find a general correlation between the motion and the HXR flux of one footpoint: the source moves during times of strong HXR emission but slows down during times of low emission. This is consistent with more energetic electrons being produced and therefore more HXR emission when there is more rapid reconnection, as observed as more rapid apparent motion of footpoints. At the same time, there are also other energy releases, in Hα emission and in long-lived soft X-ray emission, which appear related to reconnection but without HXRs and electron acceleration. How and why particle acceleration occurs is still unkown at present; a treatment of these questions and of flare energetics will be left for future analyses.

REFERENCES

Emslie, A. G., Kontar, E. P., Krucker, S., & Lin, R. P. 2003, ApJ, 595, L107
Fletcher, L., & Hudson, H. S. 2002, Sol. Phys., 210, 307
Lin, R. P., Schwartz, R. A., Pelling, R. M., & Hurley, K. C. 1981, ApJ, 251, L109
Lin, R. P., et al. 2002, Sol. Phys., 210, 3
———. 2003, ApJ, 595, L69
Øieroset, M., Lin, R. P., Phan, T. D., Larson, D. E., & Bale, S. D. 2002, Phys. Rev. Lett., 89, 19

Priest, E. R., & Forbes, T. G. 2002, A&A Rev., 10, 313
Qiu, J., Lee, J., Gary, D. E., & Wang, H. 2002, ApJ, 565, 1335
Sakao, T. 1994, Ph.D. thesis, Univ. Tokyo
Sakao, T., Kosugi, T., & Masuda, S. 1998, in ASSL Vol. 229, Observational Plasma Astrophysics: Five Years of *Yohkoh* and Beyond, ed. T. Watanabe, T. Kosugi, & A. C. Sterling (Boston: Kluwer), 273
White, S. M., Krucker, S., Shibasaki, K., Yokoyama, T., Shimojo, M., & Kundu, M. R. 2003, ApJ, 595, L111